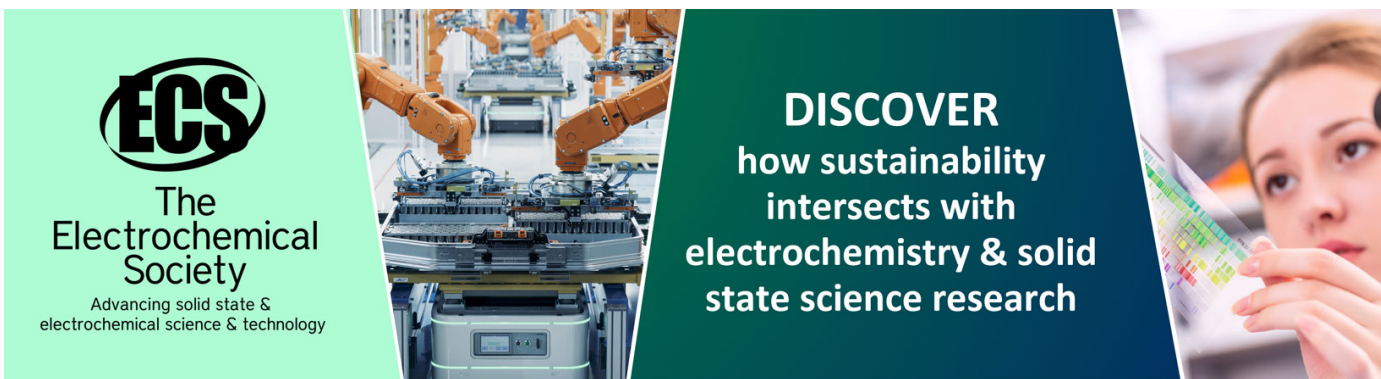SISSA

PAPER

Comparison between conventional Si and new generation of SiC detector for high proton energy spectrometry

To cite this article: L. Torrisi *et al* 2024 *JINST* **19** P04032

View the article online for updates and enhancements.

Comparison between conventional Si and new generation of SiC detector for high proton energy spectrometry

L. Torrisi ,[a,*] **V. Havranek,**[b] **A. Mackova,**[b] **L. Calcagno,**[c] **A. Torrisi** [d] **and M. Cutroneo** [a,b]

[a]*Dipartimento Scienze Fisiche-MIFT, Università di Messina,*
S. F. d'Alcontres 31, 98166 Messina, Italy

[b]*Nuclear Physics Institute — AS CR,*
Hlavní 130, 25068 Řež, Czech Republic

[c]*Dipartimento di Fisica ed Astronomia, Università di Catania,*
Via S. Sofia 64, 95135 Catania, Italy

[d]*Department of Medicine and Surgery, Kore University of Enna,*
Cittadella Universitaria, 94100 Enna, Italy

E-mail: lorenzo.torrisi@unime.it

ABSTRACT: A SiC Schottky diode and a Si surface barrier detector have been compared during Rutherford backscattering spectrometry (RBS) using 2–3 MeV proton beams. Both detectors are suited to detect high energetic ions with high-energy resolution for spectroscopic analysis.

The correlations between the detector parameters and the surface passivating layers, ion energy and current dependence, ion penetration depth, detection efficiency and energy resolution, are outlined.

Comparative RBS analysis performed using SiC and Si detectors has been investigated to highlight the advantages and disadvantages of the use of SiC with respect to the traditional Si junction detector. RBS spectrometry has been carried out using projectiles of proton incident on different targets to analyse their composition and thickness by the detection of the backscattered ions revealed by Si and SiC detectors.

---

*Corresponding author.

Contents

1   Introduction

The first synthesis of a silicon-carbon composite dates back to 1824 as reported by Berzelius [1].

Typically, SiC is described as a unit made of one Si atom with 4 C atoms forming a tetrahedral structure. This 'module' is the same for all SiC polytypes, which differ only for the variations in the order of the stacking. Currently, it is possible to classify 200 crystal polymorphs by cubic (C), hexagonal (H), and rhombohedral (R) lattice symmetry. The number of layers in the stacking sequence usually is written in front of the symmetry letter, resulting in 3C-SiC, 4H-SiC, and 6H-SiC4H-SiC [2].

Our research group has already carried out studies using SiC detectors with a surface area from $2\,mm^2$ up to $9\,mm^2$, with a maximum depletion depth of 80 microns and with different surface metallization. They have been used to detect various types of ions, both low and high energy, from about 10 keV to about 10 MeV, as reported in the literature [3–6].

Rutherford backscattering spectrometry (RBS) is a non-destructive nuclear method for elemental concentration, thickness measurements and depth profiles on different materials. It is conducted by the detection of the number and energy distribution of ions typically helium with energy of 2–3 MeV backscattered from atoms located at the surface of the investigated material. The detection of the backscattered ions is routinely conducted using Si detectors. However, the use of SiC detectors although display energy resolution and sensitivity comparable with that of Si barrier detectors further benefits like higher resistance to high temperature, high radiation damage, intense visible light, and high ion absorbed doses have been referred [7, 8].

Generally, the surface barrier radiation detectors employed for high-resolution charge-particle spectrometry are represented by p-n junction partially depleted Si detectors. They have a minimum depletion depth of the order of 1000 μm and an active surface from $25\,mm^2$ to more than $100\,mm^2$, as well as those produced by Ortec [9]. They are biased with a low reverse bias of the order of 50 V and their reverse current is of the order of 100 nA. Their surface is covered with about 10 nm Au and the Si dead layer thickness is of the order of 20 nm. Their energy resolution for 5 MeV alpha particles is of the order of 0.05 % [9].

For comparison, the main characteristics of our used SiC Schottky detector have been listed as follows: an active depletion layer of the order of 80 μm at a reverse bias of 500 V with a reverse current of about 10–100 pA. Despite Si, having a gap energy of about 1.1 eV, the visible light does not disturb the SiC detection because its energy gap is 3.3 eV. Commonly, they have an active area of the order of some mm^2 and a surface covered by Ni_2Si with a thickness between 20–200 nm. The dead layer of Schottky SiC is of the order of 20 nm and the SiC energy resolution is slightly worse than that of silicon junction detectors [10].

Table 1. Some physical properties of SiC and Si semiconductor materials.

Material property	4H-SiC	Silicon	Detector property	SiC	Si
Crystal structure	Hexagonal	Diamond	Proton stopping power (2 MeV)	38.94 keV/μm	26.21 keV/μm
Band gap (eV)	3.26	1.12	Proton Range (2 MeV)	31.58 μm	47.51 μm
Density (g/cm^3)	3.21	2.33	Proton energy loss in the dead layers (2 MeV)	14.1 keV	1.41 keV
Electron mobility (cm^2/V s)	800–1000	1450–1500	Detection efficiency (2 MeV H$^+$)	100 %	100 %
Holes mobility (cm^2/V s)	100–115	450–600	Reverse bias	−200 V	+50 V
Breakdown electric field (MV/cm)	2.2 – 4.0	0.2 – 0.3	Depletion layer (−200 V)	30 μm	1000 μm
Mean e-h pair energy (eV)	7.78	3.63	Active surface area	9 mm^2	25 mm^2
Thermal conductivity (W/cm °C)	3.0 – 5.0	1.5	Subtended solid angle	2.1 mstr	3.2 mstr
Max working temperature (°C)	1240	300	Surface metallization	Ni$_2$Si (200 nm)	Au (10 nm)
Effective atomic number	12.54	14	Reverse current	0.1 nA	10 nA
Displacement energy (eV)	25	13–20	Junction type	Schottky	p-n

SiC represents an innovative detector able to detect UV and X-rays, and energetic electrons and ions, which can be used for different applications, from plasma monitoring spectroscopy to time-of-flight measurements, from high-power diodes and transistors to different biomedical applications [11–13]. Their detection efficiency is limited by the surface dead layer and by their limited active depletion layer.

This paper aims to compare the performance exhibited by SiC with that obtainable using classic Si barrier surface detectors throughout the proton RBS analysis.

Accordingly, proton beams at 2 and 3 MeV energies incident on different solid targets have been placed in high vacuum, recording the Rutherford backscattered particles with SiC and Si both placed at an angle of 165°.

Table 1 lists some physical properties of the 4H-SiC and of the Si as well as further properties of the SiC Schottky and Si p-n junction surface barrier used detectors.

2 Materials and methods

The proton beams (2–3 MeV) have been obtained at the 3 MV Tandetron accelerator of the Nuclear Physics Institute (NPI) in Rez [14]. The proton current was almost always kept at 10 nA, but tests were also done with currents between 0.1 nA and 50 nA. The proton spot was of about 0.5 mm^2.

Used targets were thick samples of Si (300 µm thick) without and with covered thin films. The most important targets used for this investigation were those prepared by physical vapor deposition (PVD) in a high vacuum consisting of 100 nm Au thin film deposited on a Si substrate and that prepared with multi-thin films deposition of Au (130 nm)/Ag (98 nm)/Cu (55 nm) deposited on a Si substrate.

The silicon detector was an Ortec (A series) partially depleted silicon surface barrier with 25 mm^2 surface area, biased at 50 V, with 100 µm active depth [6]. Its reverse current was about 10–20 nA. The Si detector was placed at 89 mm distance from the target and at 165° backscattering angle, covering a solid angle of 3.2 mstr.

The SiC Schottky detector was realized at ST-microelectronics, in collaboration with CNR-IMM of Catania (Italy) [15], where were used lithographic processes to realize the Schottky junctions and the Ohmic contacts of the surface and of the device's back face. The diode was used reversely biased through a protection resistance of 100 kΩ at a voltage of −200 V. At this bias the reverse current of the diode was 0.1 nA, as measured with a Keythely instrumentation at room temperature and in vacuum (10^{-6} mbar). SiC was realized on-type 4H-SiC epitaxial layers, 80 mm thick with 10^{14} cm^{-3} dopant concentration onto a n-type heavily doped substrate. Ohmic contacts on the sample back side were formed by sputtering a 200 nm thick nickel film. The front contacts were obtained by sputtering deposition of a Ni thick film and performing a rapid thermal processing at 700°C producing the formation of Ni$_2$Si 200 nm thick. The active surface was 3 mm × 3 mm, characterized by the 200 nm Ni$_2$Si dead layers having a density of 7.4 g/cm^3. The SiC detector was placed at 65 mm distance from the target and at 165° backscattering angle, covering a solid angle of 2.1 mstr.

The low detection solid angles used in the experiment and the low proton current avoid any pile-up effect in the acquired RBS spectra.

Figure 1(a) shows a photo of the used SiC detector, figure 1(b) that of the used Si detector. Figure 1(c) reports a geometrical sketch of the SiC assembly structure employed in this experiment and figure 1(d) is a scheme of the experimental setup geometry of the two used detectors, the Faraday cup used for the ion beam current and of the incident ion beams.

Figure 2 reports the theoretically calculated detection efficiency for the used SiC detector relatives to protons and helium beams versus ion energy, according to the literature [10]. The low energy threshold was calculated on the base of the protons and alpha particles energy loss in the dead layers of the SiC detector (Ni$_2$Si metallization), while the high energy threshold on the base of the active region (80 microns depth). It is assumed that 100 % efficiency is reached when the particle deposits all its energy in the active region.

A detection efficiency above 80 % is evaluated, approximately, for the proton's energy in the range of 200 keV to 4 MeV and the alpha particle's energy in the range of 700 keV to 10 MeV.

Figure 3 shows a block scheme of the detection electronics used for SiC and Si ion detection for RBS spectrometry. It is based on a preamplifier (Ortec mod. 142 A), a linear amplifier (Ortec mod. 672) with 0.1 µs shaping time and a very compact digital Multi-Channel Analyzer (MCA, Amptek MCA-8000D) to digitize the analogical input signal and to acquire the RBS spectra.

RBS analysis performed using 2 and 3 MeV proton beams was carried out taking into consideration the kinematic backscattering factor depending on the energy of the backscattered particle with respect to that of the incident one and by considering the differential scattering Rutherford cross sections in the laboratory system [16, 17].
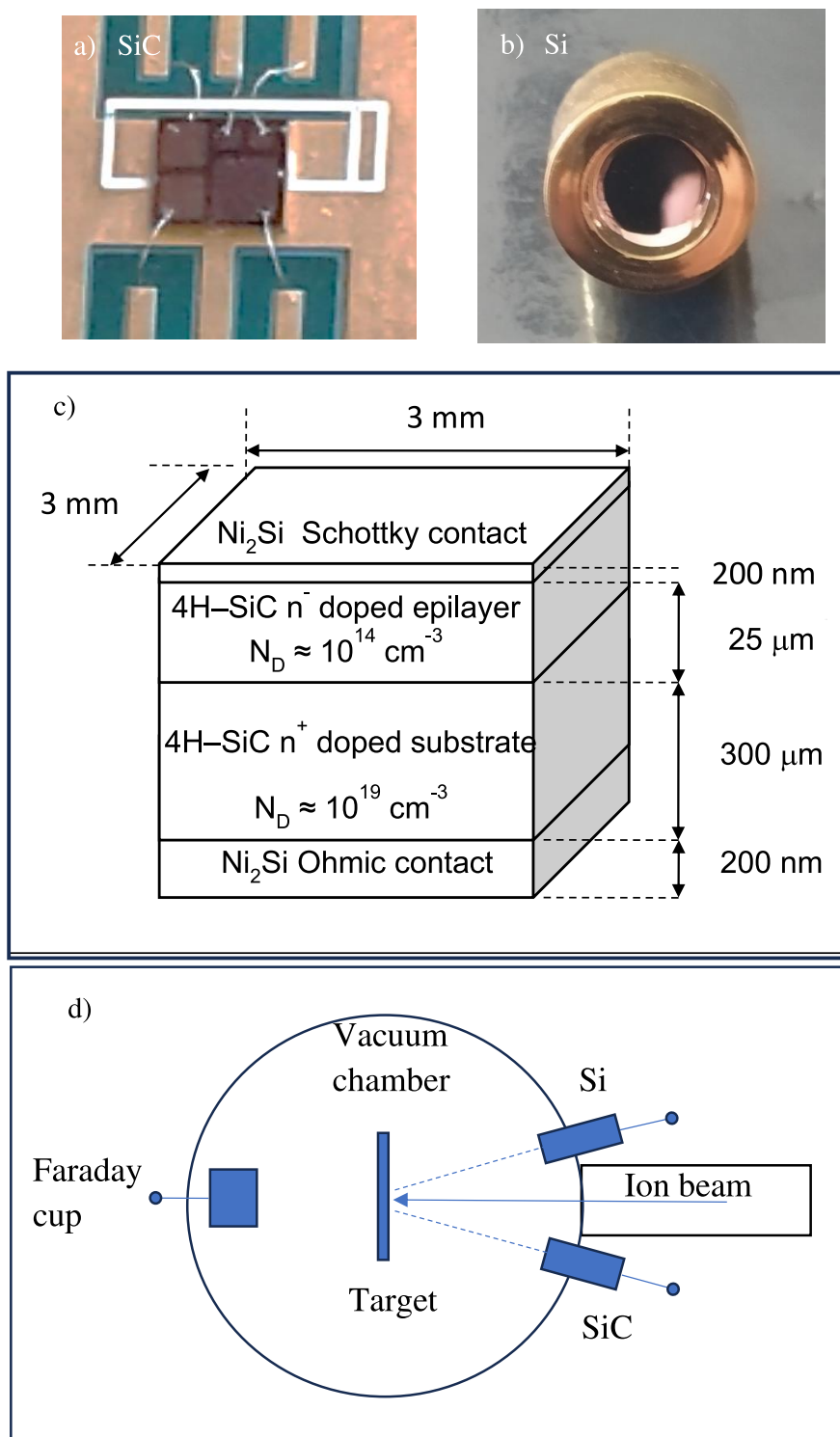
Figure 1. Photo of the SiC (a) and of the Si (b) detectors, scheme of the SiC detector assembly (c) and geometry of used detectors with respect to the incident ion beam (d).
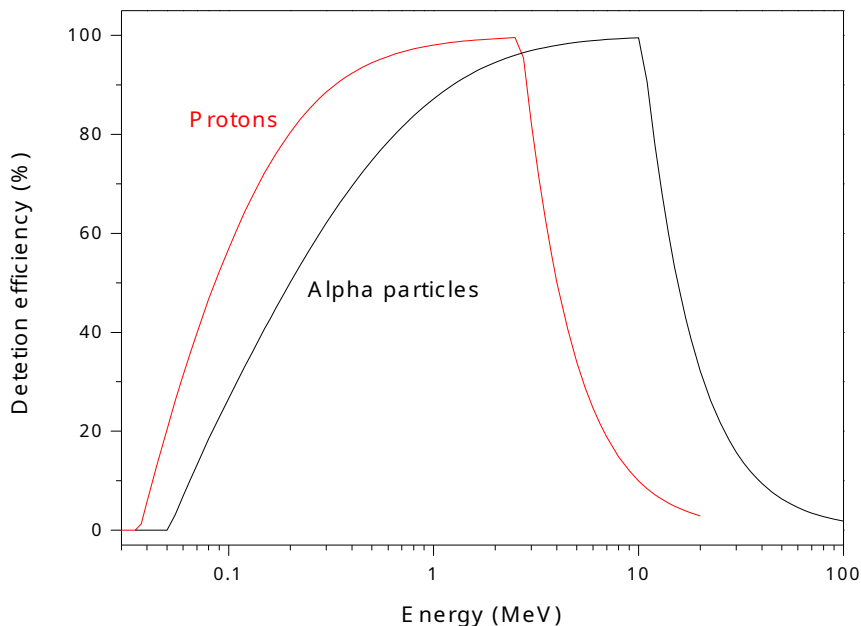
Figure 2. Detection efficiency of SiC detector versus proton and helium beam energy.
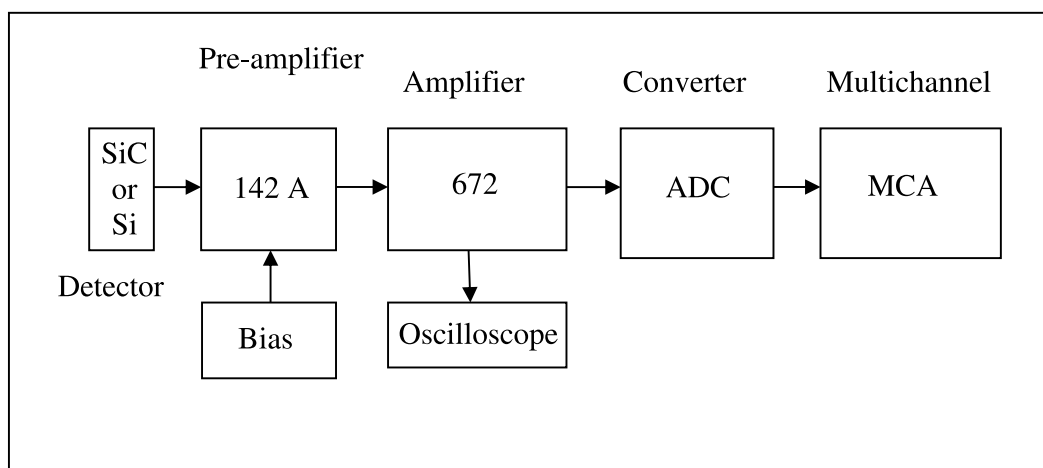

Figure 3. Scheme of the electronic detection system for SiC and Si detectors.

3 Results and discussion

A preliminary measure was accomplished at the energy resolution of the SiC and Si-Ortec detector by using a traditional 3-peak alpha source composed of ^{239}Pu, ^{241}Am and ^{244}Cm emitting at 5.15 MeV, 5.48 MeV and 5.80 MeV, respectively [18]. The relative activities of the three radioactive sources of Pu, Am and Cm are in the ratio 1:0.65:0.23, respectively. Therefore, the maximum activity is that of Pu and the minimum activity is that of Cm.

Figure 4 compares the alpha spectra acquired using the SiC (a) and the Si (b) detectors. The peak yields (peak areas) are in good agreement with the three-source activities.

The measured average energy resolution for the three alpha energies for SiC and Si detectors is 0.22 % and 0.038 %, respectively, in agreement with the literature [10].
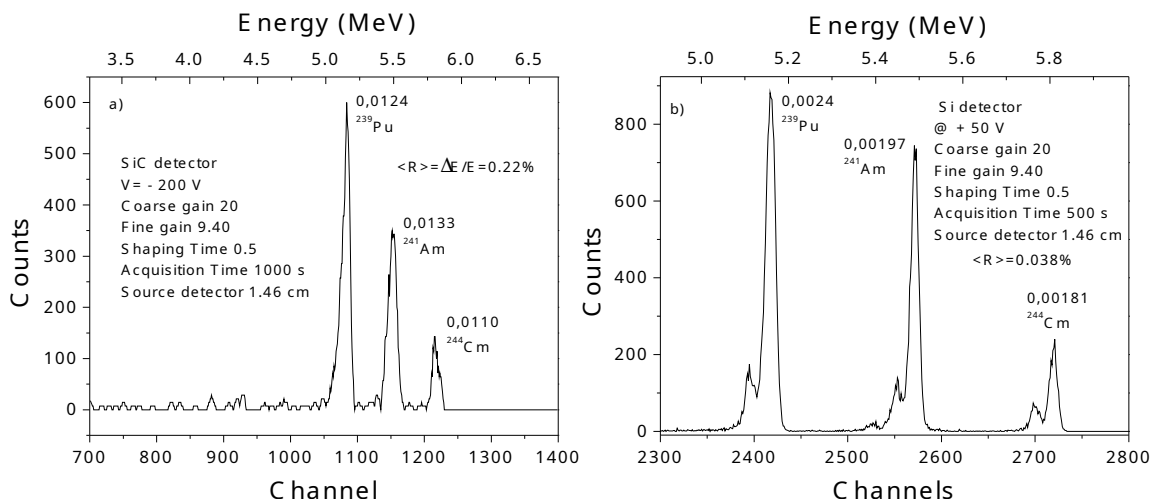
Figure 4. Three peaks alpha source detected by using SiC (a) and Silicon (b) detectors.

Such values also contain the energy straggling of the alpha particles in the surface metallization (200 nm Ni_2Si for SiC and 20 nm Au for Si) and the noise due to the electronic detection system.

Some typical RBS spectra obtained using $E_p = 2.0$ MeV H^+ ions with a current of 10 nA, acquired in 1000 s with SiC (left) and Si (right) detectors, in the same irradiation experimental conditions (SCS), have been compared between them to investigate on the obtainable spectra differences.

The calibration procedure of the MCA performed using the two detectors has given a calibration factor corresponding to 8.59 keV/ch and 4.04 keV/ch for the SiC and Si RBS spectra, respectively.

The peak width (full width at half maximum FWHM) in MeV is shown next to each peak (figure 4).

Figure 5 reports the comparison between the SiC (a) and the Si (b) spectra relative to the analysis of a Si target substrate covered by 100 nm Au thin film. The different counts of the vertical scale, minor for the SiC detector with respect to the Si one, are due to the minor subtended solid angle and to the different energy needed to produce the electron-hole pairs.

At the backscattering angle (165°), the kinematic factors for Si and Au are 0.8683 and 0.9801, respectively [16]. Thus, the corresponding backscattered maximum proton energies from the Si and Au surface are 1.734 MeV and 1.960 MeV, respectively.
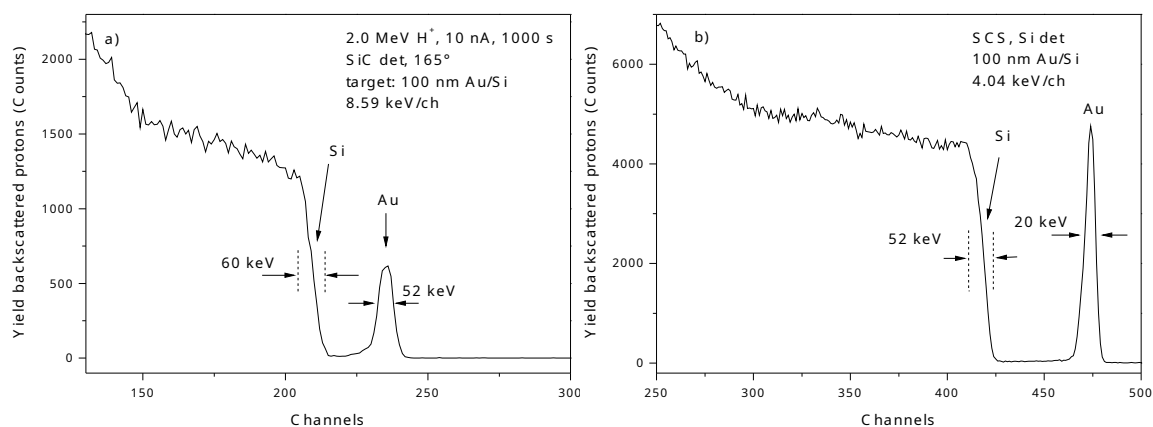

Figure 5. 2.0 MeV H^+ RBS spectra of 100 nm Au/Si target acquired using SiC (a) and Si (b) detectors.

It is possible to observe that the RBS step signal related to Si target, acquired using the SiC detector, is wide 60 keV, while the width (FWHM) of the peak related to the Au thin film is equal to 52 keV.

The width for Si is calculated taking into consideration the channel position of the minimum and maximum edge of the Si backscattered protons ed evaluating their difference in terms of energy from the given energy calibration.

Moreover, it is also possible to observe that the RBS step signal related to Si target, acquired using Si detector, is wide 52 keV, while the width (FWHM) of the peak related to the Au thin film is equal to 20 keV.

Consequently, the better Si detector energy resolution is confirmed also by the detected RBS spectra analysing the Au/Si target.

Further leverage of the Si detector is revealed by the Au signal yield (peak area) with respect to the Si intensity (step high) whose ratio is 7.22, against that shown in the SiC spectrum where the ratio corresponds to 3.48. This dissimilarity is mainly due to the different pair energy generation and proton energy loss in the two semiconductor detectors.

The above-reported spectra were acquired also using proton currents from 0.1 nA up to 50 nA. In this range the proton backscattered yield (counts) depends linearly on the ion current, thus the yield reported in figure 5(a), for example, duplicates by doubling the current to 20 nA and keeping the acquisition time constant. At higher currents, a dead time appears on the MCA acquisition data, especially for the SiC detector, probably as a consequence of its minor time responsivity produced by the minor carrier mobility with respect to the Si semiconductor (see table 1).

Another useful comparison between 2.0 MeV protons RBS spectra acquired using SiC (a) and Si (b) is observable by the spectra comparison reported in figure 6. It concerns the analysis of a target constituted by thin three-multilayer films covering a Si wafer constituted by Au (130 nm)/Ag (98 nm)/Cu (55 nm)/Si substrate.
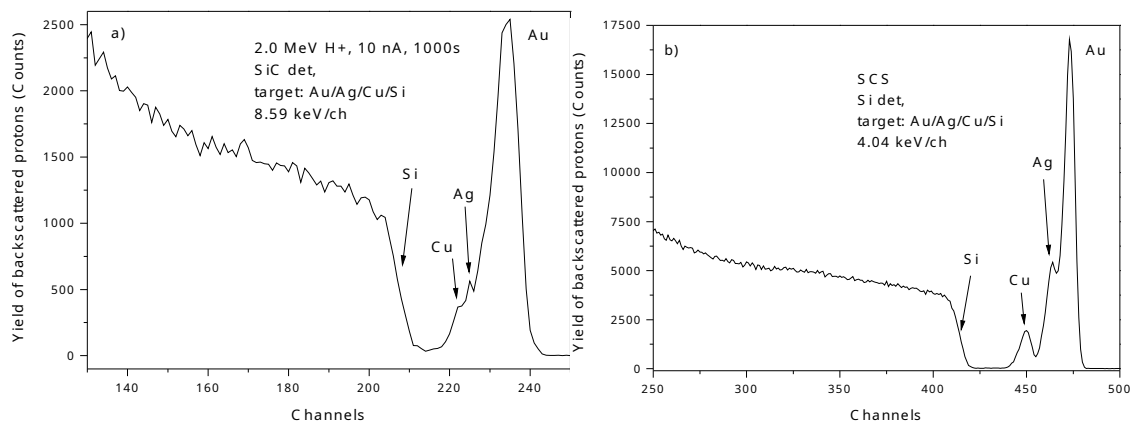

Figure 6. 2.0 MeV H⁺ RBS spectra of Au/Ag/Cu/Si target acquired using SiC (a) and Si (b) detectors.

Also, in this case, it is possible to observe better qualitative element separation using the Si detector instead of the SiC one. In this last case, the three peaks are barely distinguishable and are represented by a single ion peak which requires a careful deconvolution to highlight the individual contributions, while they result well separated using the Si detector. The higher pair energy generation in SiC, about double with respect to Si, the higher proton energy loss in the SiC detector, having a higher density, the higher detector energy resolution and proton energy straggling in the thicker surface

metallization of Ni_2Si determine a less spectrum energy resolution and in detected backscattered ion yield. In fact, also the thin film peak area to silicon step high ratio is minor of about a factor of two for SiC with respect to Si one.

Let us now try to understand what happens if we increase the energy of the RBS analysis proton beams to 3.0 MeV. We use the same previous target of Au/Ag/Cu/Si using the same current of 10 nA and acquisition time of 1000 s and record the RBS spectra with the same two detectors. In this case, by using the kinematic factor for Si and Au, the maximum backscattered proton energy corresponds to 2.60 MeV and 2.94 MeV, respectively, as reported in figure 7.

Although the increase in energy of the protons leads to a better energy resolution of the element peaks seen by the RBS via the SiC detector (a), the spectra of the Si detector (b) always remain better highlighted and resolved.
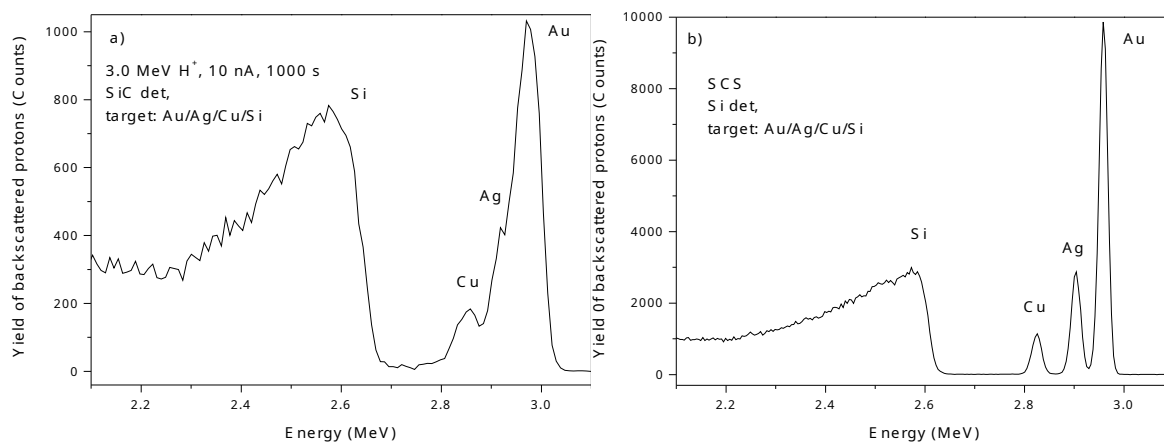

Figure 7. 3.0 MeV H^+ RBS spectra of Au/Ag/Cu/Si target acquired using SiC (a) and Si (b) detectors.

Based on the results presented we can consider the Ortec Si detector certainly better than the SiC detector used, however, the latter may present some advantages compared to the Si detector in the following cases:

1) Ion irradiation of luminescent targets emitting in the visible region under bombardment, resulting in a significant disturbance of the RBS spectra acquired using Si detector due to the considerable background present in such detectors. This effect cannot be seen by SiC detectors due to their greater energy gap, in agreement with the literature [19].

2) Execution of RBS analyses in high temperature conditions which increases the reverse current of the Si detectors deteriorating the spectra energy resolution but which in practice are almost irrelevant on SiC detectors which also operate at high temperatures, according to the literature [20].

3) At high absorbed doses, long irradiation times and heavy ion detection, there is less damage to SiC detectors with respect to the Si one which loses its better energy resolution. This effect is due to the higher atomic binding energy of the SiC structure with respect to the Si one. Therefore, the average life of SiC detectors is greater than those based on Si which at high doses and for heavy ions worsens its energy resolution, according to recent literature data [19, 21].

In many experiments, SiC detectors may be used for high-temperature applications. For example, SiC may be used to monitor the ions, electrons and photons emitted from laser-generated plasma, during high-temperature plasma production, and during pulse laser deposition [11, 22, 23].
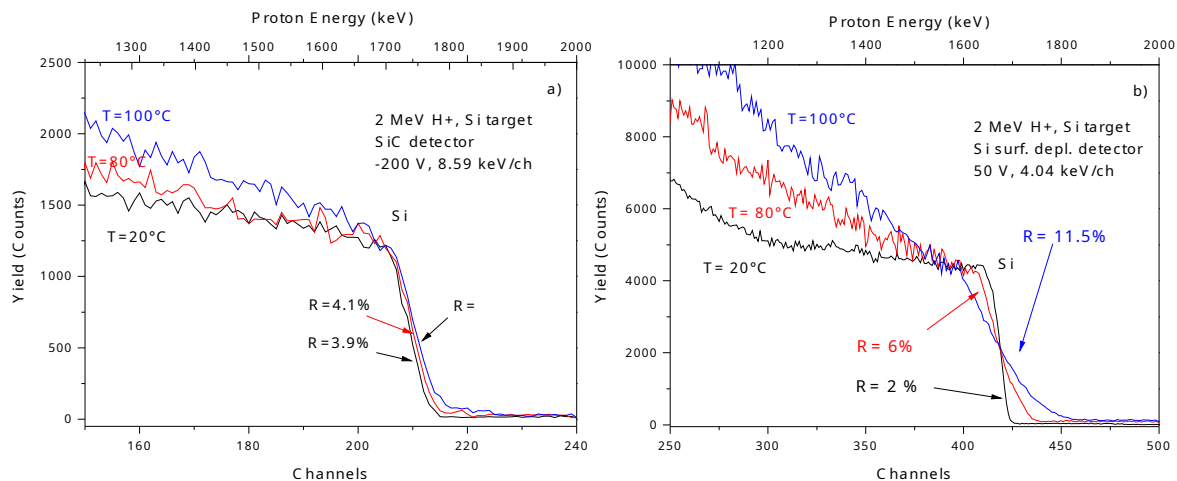
Figure 8. 2.0 MeV protons RBS spectra of pure silicon target at three different temperatures for SiC (a) and Si (b) detectors.

Preliminary measurements of energy resolution using the 2.0 MeV proton RBS spectra relative to a pure Si target have been performed with the SiC and Si detectors placed in a vacuum at three different temperatures, 20 °C, 80 °C and 100 °C, as reported in figure 8(a) and 8(b), respectively.

Measurements have demonstrated that the energy resolution increases significantly in the case of the Si-Ortec detector due to its high increment of the leakage current. Si detectors have a bad energy resolution at 100°C and cannot operate at a temperature of about 250–300°C. Instead, in the case of SiC its energy resolution for proton beams remains near constant from room temperature up to about 100°C, as reported in the plot of figure 8, in agreement with literature data [20, 24].

Albeit in a less accurate mode, the energy resolution of the two detectors was evaluated by the energy width of the step in the yield of the RBS signal relative to silicon target, i.e. at 1734 MeV of proton backscattering. This evaluation, obtained from the extrapolation lines between the bottom, the Si signal, and the inclination of the step, was carried out by varying the temperature at which the two detectors were placed under vacuum. The results are reported in figure 9, indicating that at room temperature generally the Si energy resolution is better than SiC, but increasing the temperature the high leakage current deteriorates it to values worse than those of SiC.

It is also important to keep in mind that the SiC detector we use represents only a prototype that should be further optimized to be able to be used regularly for RBS spectroscopic analyses. For example, by reducing the thickness of the surface metallization, using low-density surface metallization and more adapt detection electronics its energy resolution could be improved.

The research activity concerning the use of SiC and Si detectors versus the type of ion beam, target composition and temperature is in progress and will be better reported in the next paper.

4 Conclusions

The SiC-Schottky detectors are extensively exploited for plasma monitoring analysing the emitted UV, X-rays, energetic ions and electrons. Additionally, they are useful for measurements of time-of-flight during laser-matter interaction, for gas puff X-ray emission for innovative microscopy, for high- power diode devices and many microelectronic applications.
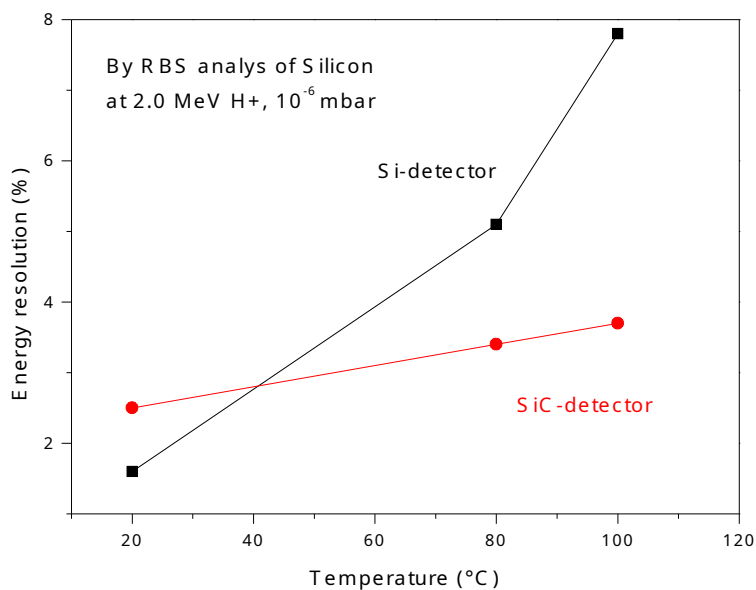
Figure 9. Energy resolution by three peak alpha source versus temperature for Si and SiC detectors.

This paper has investigated the possibility of applying SiC for RBS spectrometry using proton beams, similar to a previous contribution that referred to the use of standard helium beams.

We have demonstrated that SiC diodes detect protons with energy in the range of about 50 keV up to about 10 MeV with a sufficient energy resolution to be used for proton spectrometry, like silicon detectors employable for qualitative and quantitative RBS analyses. The used SiC prototype has a surface-active area of 3 mm × 3 mm, with 200 nm thickness in Ni_2Si alloy, 80 microns active region depth, using a bias of −200 V at which this active region is reduced to about 30 microns depth.

RBS measurements demonstrated that the SiC energy resolution is comparable to that of Si, although, at room temperature, Si appears to have an energy resolution better than a factor 3.5 with respect to SiC.

Si-barrier detectors produced by Ortec show high energy resolution and are realized for ion spectrometry such as RBS by helium and proton beams. They have a thin Au surface metallization and thin dead layers to reduce the ion energy loss and straggling of the incident ions. The Ortec preamplifier and amplifier are able to enhance the signal to noise ratio and acquire RBS spectra with minimum background.

SiC Schottky detectors do not have better energy resolution than Si but offer some important advantages. It consists in the higher energy gap, that permits to be transparent to visible radiation and to be used also in presence of high visible radiation. SiC shows a lower reverse current, of about two order magnitude lower with respect to Si; it is radiation resistant due to the higher bonding energy Si-C with respect to Si-Si, making it possible to use even in harsh conditions, such as plasmas, high visible light intensity, and high temperatures. SiC can be employed to monitor on-line ion beams, plasmas radiation emission and lasers interacting with solids.

The SiC use can be optimized not only at low ion energy but also at high ion energy, increasing the active depth of the sensible detector region, enhancing its detection efficiency for low and high ion energies, improving its signal-to-noise ratio with optimized preamplifier electronics, it can be used also at relatively high temperatures maintaining near constant its energy resolution.

Acknowledgments

References

[1] J.J. Berzelius, *Untersuchungen über die Flussspathsäure und deren merkwürdigsten Verbindungen*, *Annalen Phys.* **77** (1824) 169.

[2] T. Kimoto and J.A. Cooper, *Fundamentals of Silicon Carbide Technology: Growth, Characterization, Devices, and Applications*, John Wiley & Sons, New York (2014) [`DOI:10.1002/9781118313534`].

[3] L. Torrisi et al., *Single crystal silicon carbide detector of emitted ions and soft x-rays from power laser-generated plasmas*, *J. Appl. Phys.* **105** (2009) 123304.

[4] M. Cutroneo et al., *High performance SiC detectors for MeV ion beams generated by intense pulsed laser plasmas*, *J. Mater. Res.* **28** (2013) 87.

[5] L. Torrisi, M. Cutroneo and A. Torrisi, *SiC Measurements of Electron Energy by fs Laser Irradiation of Thin Foils*, *Micromachines* **14** (2023) 811.

[6] J.K.N. Lindner, *Formation of SiC Thin Films by Ion Beam Synthesis*, in *Advanced Texts in Physics*, W.J. Choyke, H. Matsunami and G. Pensl, eds., Springer Berlin Heidelberg (2004), pp. 251–277 [`DOI:10.1007/978-3-642-18870-1_11`].

[7] L. Torrisi et al., *SiC detector for high helium energy spectroscopy*, *Nucl. Instrum. Meth. A* **903** (2018) 309.

[8] L. Torrisi et al., *SiC Detector for Sub-MeV Alpha Spectrometry*, *J. Electron. Mater.* **46** (2017) 4242.

[9] Ortec-Ametek, *Silicon Charged Particle Radiation Detectors*, https://www.ortec-online.com/products/radiation-detectors/silicon-charged-particle-radiation-detectors /si-charged-particle-radiation-detectors-for-alpha-spectroscopy.

[10] A. Sciuto et al., *Advantages and Limits of 4H-SIC Detectors for High- and Low-Flux Radiations*, *J. Electron. Mater.* **46** (2017) 6403.

[11] A. Torrisi et al., *Calibration of SiC Detectors for Nitrogen and Neon Plasma Emission Using Gas-Puff Target Sources*, *IEEE Trans. Electron Devices* **64** (2017) 1120.

[12] T. Kimoto and H. Watanabe, *Defect engineering in SiC technology for high-voltage power devices*, *Appl. Phys. Express* **13** (2020) 120101.

[13] C.L. Frewin et al., *Silicon Carbide Materials for Biomedical Applications*, in *Carbon for Sensing Devices*, D. Demarchi, A. Tagliaferro, eds., Springer International Publishing (2014), p. 153–207 [`DOI:10.1007/978-3-319-08648-4_7`].

[14] Nuclear Physics Institute, CANAM Laboratory, Rez, Czech Republic, http://www.ujf.cas.cz/en/.

[15] CNR-IMM, Institute for microelectronics and microsystems, Catania, Italy, https://www.cnr.it/en/institute/057/institute-for-microelectronics-and-microsystems-imm.

[16] L.C. Feldmann and J.W. Mayer, *Fundamentals of surface and thin film analysis*, North-Holland, Elsevier, New York (1986).

[17] J.W. Mayer and E. Rimini, *Ion Beam handbook for Materials analysis*, Elsevier (1977).

[18] G. Espinosa and R.J. Silva, *Alpha-particle analysis of a triple isotope ^{239}Pu-^{241}Am-^{244}Cm source by nuclear track Methodology*, *J. Radioanal. Nucl. Chem.* **248** (2001) 575.

[19] T.H. Zabel et al., *The response of silicon surface-barrier detectors to light and heavy ions*, *Nucl. Instrum. Meth.* **174** (1980) 459.

[20] K. Udaykumar et al., *The effect of temperature on the behavior of semiconductor silicon surface barrier detectors*, *Radiat. Meas.* **36** (2003) 625.

[21] C. Altana et al., *Radiation Damage by Heavy Ions in Silicon and Silicon Carbide Detectors*, *Sensors* **23** (2023) 6522.

[22] D. Margarone et al., *New methods for high current fast ion beam production by laser-driven acceleration*, *Rev. Sci. Instrum.* **83** (2012) 02B307.

[23] L. Torrisi and A. Torrisi, *SiC and Ion collectors as diagnostics of laser-generated plasma at intensity of 10^{10} W/cm^2*, 2022 *JINST* **17** P04016.

[24] R.J. Grainger, J.W. Mayer and J.W. Oliver, *Temperature Behavior of P-N Junction Detectors*, *IRE Trans. Nucl. Sci.* **8** (1961) 116.